Low-Temperature Resistance Anomaly at $SrTiO_3$ Grain Boundaries: Evidence for an Interface-Induced Phase Transition

Rui Shao,[1] Matthew F. Chisholm,[2] Gerd Duscher,[2,3] and Dawn A. Bonnell[1]

[1]*Department of Materials Science and Engineering, University of Pennsylvania, Philadelphia, Pennsylvania 19104, USA*
[2]*Oak Ridge National Laboratory, Oak Ridge, Tennessee 37831, USA*
[3]*Department of Materials Science and Engineering, North Carolina State University, Raleigh, North Carolina 27695, USA*

(Received 20 April 2005; published 3 November 2005)

Variable temperature transport between 1.4 and 300 K, structural imaging, and theoretical calculations were used to characterize the properties of electrically active 24° and 36.8° [001] tilt $SrTiO_3$ grain boundaries with 0.1 at. % niobium doping. An anomaly in boundary resistance and capacitance characteristics typical of a positive temperature coefficient effect is observed. This behavior is indicative of interface-induced dipole ordering. The detailed atomic structures of these grain boundaries were determined from a comparison of *ab initio* calculations and *Z*-contrast TEM images. The number of excess electrons at the boundaries determined experimentally and theoretically agrees and is associated with the boundary structural units.

DOI: 10.1103/PhysRevLett.95.197601 PACS numbers: 77.80.Bh, 68.37.Lp, 73.40.−c

$SrTiO_3$, often regarded as a model system for perovskites, possesses unique properties that have attracted extensive research over the past decades. At low temperatures, it undergoes an antiferrodistortive phase transition at 105 K [1], a soft phonon anomaly and possible phase transition at around 37 K [2,3], as well as a transition to a superconducting state below 1 K with certain levels of donor doping [4]. These low-temperature behaviors in single crystals have been well characterized. Few studies of the effects of boundaries in bicrystal or polycrystalline $SrTiO_3$ have yet been done in this temperature range, despite the broad interest in interface mediated transport in this class of materials. It is widely believed that acceptor states at grain boundaries (GBs) give rise to local upward band bending, leading to a highly resistive depletion layer, which is phenomenologically modeled as a double Schottky barrier [5]. Recent transport measurements on reduced $SrTiO_3$ GBs have shown that a weak potential barrier exists as low as 10 K [6]. In contrast, donor-doped boundaries exhibit significant current-voltage (*I-V*) nonlinearity even at room temperature, the existence of which implies a substantially higher potential barrier at the GBs [7]. High resolution electron microscopy has been applied to imaging atomically abrupt $SrTiO_3$ GBs in an effort to determine the origin of interface charge and states [8–11]. Some reports associated charge due to localizations of excess electrons at dislocation cores, but no general conclusions have been reached regarding interface structure.

In this Letter, we report our discovery of an anomaly in GB resistance and capacitance, generally termed the positive temperature coefficient (PTC) effect, which suggests ferroelectric-type ordering induced by the oxide interface. While ferroelectricity has been observed in $SrTiO_3$ under extreme conditions (large fields [12], large stresses [13], or constrained in a thin film [14]), the GB effect is surprising. Direct probing of ferroelectric properties in donor-doped $SrTiO_3$ GBs with traditional dielectric measurements is impossible due to high sample conductivity. Our approach is to use dc and impedance transport measurements along with atomic level structural imaging and theoretical calculation to fully determine the origin of the boundary charge.

We used $SrTiO_3$ bicrystal samples (Shinkosha) containing [001] symmetric tilt GBs of either 24° or 36.8° ($\Sigma 5$) misorientation joined by diffusion bonding. *Z*-contrast transmission electron microscopy (TEM) [15] was used to determine the atomic structure. The GBs contain well ordered structural units consisting of Sr and Ti columns along the dislocation core, and no second phase or impurity segregation was detected [Figs. 1(a) and 1(b)]. First principles calculations were made as a function of oxygen occupation to determine complete boundary structure and charge density distributions. Detailed discussion of GB atomic structures is presented below. These bicrystals were doped with 0.05 weight percent (0.1 atomic percent) Nb and were sectioned into slabs 10 mm in length, 0.5 mm in thickness, and 1.6–3.0 mm in width. Indium contacts were soldered onto the surfaces for four-point dc and impedance measurements [Fig. 1(d)] in a commercial 1 k pot (Janis). Source meters and multimeters (Keithley) were used in dc transport measurements, and capacitance was measured with an impedance analyzer (HP4294A, Agilent) with an excitation amplitude = 5 mV. Hall effect measurement was performed separately (PPMS, Quantum Design) to determine the carrier concentration.

The temperature dependence of the Hall coefficient showed that carrier freeze-out does not occur between 3 and 300 K, indicating that Nb dopants act as shallow donors to the conduction band. The carrier concentration N_D at 300 K is 1.1×10^{19} cm^{-3} and is only weakly

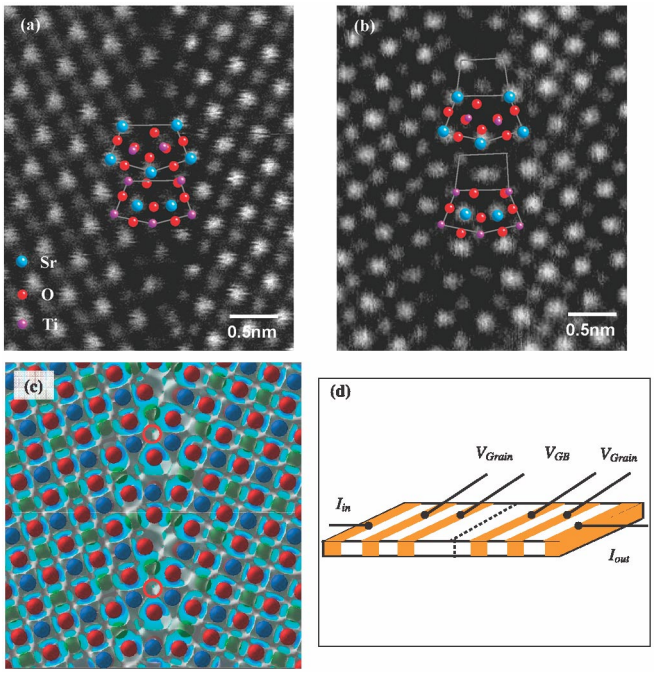

FIG. 1 (color). (a),(b) Comparison of Z-contrast images of Nb-doped $SrTiO_3$ tilt boundaries with theoretical calculations. The fully relaxed structures from *ab initio* calculations are superimposed on the Z-contrast images. The micrographs and the calculations are in excellent agreement. (c) Calculated charge density difference of a 36.8° GB. In this image: Ti (blue sphere), O (red spheres), Sr (green spheres), and O vacancies (red open circles). (d) Experimental setup for transport measurement.

temperature-dependent. Carrier mobility μ increases from 5.23 $cm^2\,V^{-1}\,s^{-1}$ at 300 K to 3.9×10^3 $cm^2\,V^{-1}\,s^{-1}$ at 3 K. In the temperature range of 40–300 K, $\mu = 10^7 \times T^{-2.5}$ $cm^2\,V^{-1}\,s^{-1}$, consistent with electron-phonon scattering [16,17].

Over the entire temperature range, I-V characteristics are nonlinear for both 24° and 36.8° GBs [Figs. 2(a) and 2(b)]. For comparison, the normalized GB resistances R_{GB} and the bulk resistance R_{Grain} are compared in Fig. 2(c). Since the bulk resistance is 2–3 orders of magnitude lower than that of the GBs, its contribution to the R_{GB} is negligible. As the temperature decreases, R_{GB} first increases to a maximum and then drops by 2 orders of magnitude to a minimum around 30 K. A slight increase occurs upon further cooling to 1.4 K. The corresponding temperatures of maximum resistance are $T_{MAX}(24°) = 163$ K and $T_{MAX}(36.8°) = 150$ K. This resistance decrease is anomalous. Transport across atomically sharp boundaries is usually described by thermionic emission of carriers across a double Schottky barrier: $J = AT^2 \exp[-(e\phi_{GB}/kT)] \times \{1 - \exp[-(eV/kT)]\}$ [5]. Zero bias resistance is estimated as $R = \frac{k}{eAT} \exp(e\phi_{GB}/kT)$. Thus, from Fig. 2(c), we can obtain the temperature dependence of the zero bias barrier height φ_{GB}. As shown in Fig. 3(a), as T decreases from room temperature, the barrier heights decrease due to the temperature dependence of the $SrTiO_3$ dielectric constant. This decrease is accelerated around $T = T_{MAX}$, indicating a decrease in boundary charge.

The anomaly is also evident in the temperature dependence of capacitance [Fig. 3(b)]. Using the abrupt junction approximation, $C_{GB}^{-1} = 2d/\varepsilon$, where ε is the dielectric constant and d is the depletion width. Above 170 K, both types of boundaries follow the Curie-Weiss law, i.e., $C_{GB}^{-1} \propto (T - \theta)$. In this temperature range, $1/\varepsilon = A_0(T - \theta)$, where the constant $A_0 = 1/80\,000/\varepsilon_0 = 1.41 \times 10^6$, according to Müller *et al.* [2]. Linear fitting yields $\theta(24°) = (23 \pm 3.8)$ K, $2A_0 d(24°) = 0.18$ for the 24° GB and $\theta(36.8°) = (20 \pm 2.4)$ K, $2A_0 d(36.8°) = 0.24$ for the 36.8° GB. We subsequently determine the width of the space charge layer: $d(24°) = 62.5$ nm

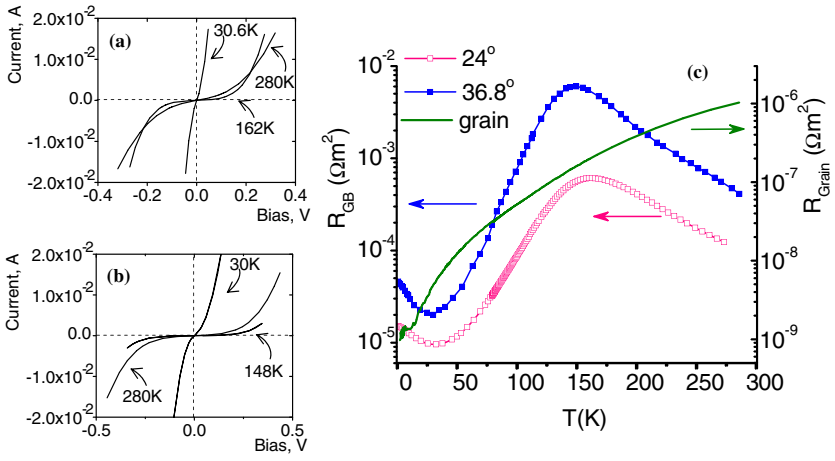

FIG. 2 (color online). I-V characteristics in GBs of both types [24° (a) and 36.8° (b)] exhibit nonlinearity throughout the whole temperature range, indicating the existence of the GB potential barrier. The GB resistances (R_{GB}) of both types show complicated temperature dependence with a maximum of R_{GB} around 140–160 K and a slow increase again as T decreases below 30 K. The resistance of single crystal R_{bulk} drops by 3 orders of magnitude from 300 to 1.4 K, characteristic of metallic behavior (c).

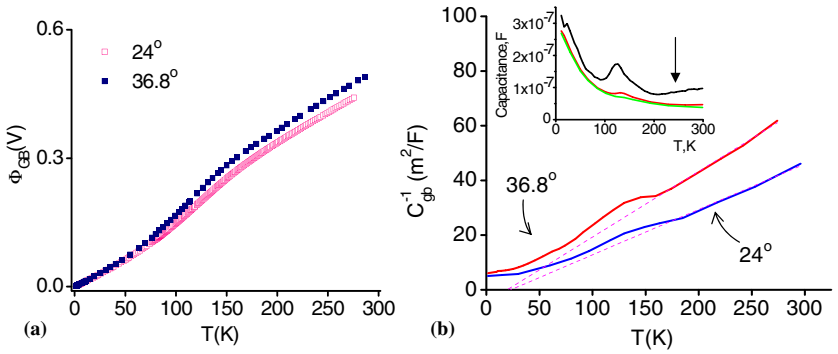

FIG. 3 (color online). (a) The GB potential barrier height φ_{GB} was obtained by fitting the R-T characteristic to thermionic emission model. The drop in φ_{GB} accelerates around 140–170 K was ascribed to the charge compensation by induced GB polarization. (b) Temperature dependence of the GB capacitance. The reciprocal capacitances of both samples deviate from Curie-Weiss law $2A_0d(T - T_0)$ (dashed lines) near the temperature for maximum resistance. Inset: Capacitance of a 36.8° GB measured at 1, 5, and 10 kHz (from top to bottom).

and $d(36.8°) = 86.8$ nm, and the boundary charge: $Q_{GB}(24°) = 0.22$ C/m^2 and $Q_{GB}(36.8°) = 0.31$ C/m^2 at 300 K. Using the structural periodicity described below, the charge per periodic structure in number of electrons for the 24° boundary is 1.0 and for the 36.8° boundary is 0.87.

To correlate the structures and properties of donor-doped GBs, it is instructive to determine the origin of the boundary charge by combining Z-contrast imaging and *ab initio* density functional theory calculations. The VASP package for *ab initio* calculations using the revised Perdew-Burke-Ernzerhof general gradient approximation with projector augmented wave potentials was used with a k-point sampling comparable to an $8 \times 8 \times 8$ mesh in a SrTiO3 unit cell [18].

The results of the calculations of fully relaxed structures are superimposed on the experimentally determined structure in Figs. 1(a) and 1(b). The generalized structure of $SrTiO_3$ [001] tilt boundaries consists of pentagonal defect units containing two cation columns. The pentagons are formed on both the SrO and TiO_2 sublattices. The 36.8° GB [Fig. 1(a)] is seen to contain only these defect units. The 24° GB contains an additional heavily distorted unit cell-like structural unit between the pentagons [Fig. 1(b)] to accommodate the different tilt angle. The details of these structures in Nb-doped $SrTiO_3$ differ from those of previous observations of GBs in undoped $SrTiO_3$, by a larger distance between the cation columns in the pentagonal units [10,19]. The calculations show that fully occupied cation columns in the units produce low energy structures. The GB energy can be further reduced by removing an oxygen column from the pentagonal unit containing two Ti-O columns. This structure also yields the best match to the experimentally observed boundary. This result agrees well with the interface charge determined from transport measurements: one electron per boundary repeat unit, and suggests that the charge originates from the oxygen deficient pentagonal unit containing two Ti-O columns.

Another result of the calculations is that all unit cells have a tetragonal distortion of about 20 pm along (100) consistent with the experimental low-temperature structure. Near the grain boundary, these distortions are oriented nearly perpendicular to the boundary plane. Furthermore, the theoretical charge density difference plot in Fig. 1(c) shows evidence of polarization with dipoles in the interface compensating direction as a result of oxygen vacancies. Polarization is evident in the asymmetric charge distribution around the atoms.

The hundredfold decrease in GB resistance is a clear indication that the interface charge is compensated by alignment of dipoles. In fact, Fig. 2(c) implies the classic positive temperature coefficient of resistance response. These observations can be explained as follows. There is a cubic to tetragonal phase transition that occurs at 105 K for pure crystals but is a function of composition. Above the structural phase transition, the temperature dependence is due to the temperature dependence of the dielectric constant. At the transition, either the local field or the local strain alters the energy landscape such that dipole alignment occurs. A similar conclusion was drawn by Petzelt *et al.* [20] based on Raman shifts in ceramics. This induced polarization P_S perpendicular to the boundary plane reduces the boundary charge Q_{GB} to $Q_{GB} - 2P_S$. Unlike the PTC effect in $BaTiO_3$, the drop in resistance is not abrupt [21]. The broad transition is explained in terms of a charge-induced phase transition that involves local dipole alignment, because in this case the transition is of second order. Furthermore, the nonlinearity of I-V curves at all temperatures indicates incomplete charge screening, consistent with the picture of induced polarization. Below the phase transition, the correlation between the electric field E and the polarization near the GB, P_S, is nonlinear. According to Landau-Devonshire theory, $E = A(T)P_S + B(T)P_S^3$, where $A = A_0(T - \theta)$ corresponds to the paraelectric behavior. To first order approximation, C_{GB}^{-1} is given by [22]

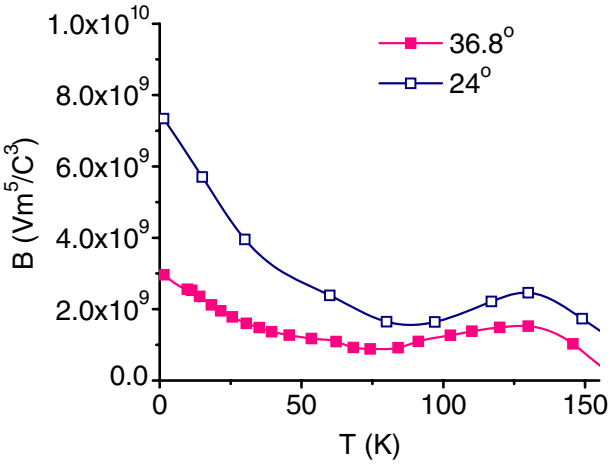

FIG. 4 (color online). Temperature dependence of B was calculated using Eq. (1).

$$C_{\mathrm{GB}}^{-1} = 2A(T)d + B(T)Q_{\mathrm{GB}}^{2}d/2. \quad (1)$$

Using A_0 and θ calculated before, the nonlinear coefficient B is that shown in Fig. 4. At 1.4 K, B is 7.3×10^9 V m^5 C^{-3} for 24° GB and 3.0×10^9 V m^5 C^{-3} 36.8° GB, which is in good agreement with that reported on $SrTiO_3$ thin films in terms of the order of magnitude [23].

The low-temperature trend in the boundary capacitance is very interesting. If the entire boundary plane is polarized, then the capacitance should decrease as the temperature drops below the "bump" corresponding to the phase transition, as observed in $BaTiO_3$. This contrasts our observation [as shown in the inset in Fig. 3(b)]. If only a portion of the boundary plane is aligned, then the measured capacitance is the sum of the capacitances C_F and C_P corresponding to two phases. The observed increase at the lowest temperatures is then due to the dominance of C_P, which still follows the Curie-Weiss law (or, more precisely, the Barrett formula [24]).

To summarize, low-temperature measurements reveal an anomaly in transport properties that results from boundary-induced dipole alignment in $SrTiO_3$. This conclusion is supported not only by resistance and capacitance measurements but first principle calculations and earlier Raman studies. The second order nature of the charge compensation with phase transformation and "patchy" incomplete screening are consistent with ferroelectric dipole interactions in $SrTiO_3$.

R. S. and D. A. B. acknowledge the financial support from the Department of Energy under Contract No. DE-FG02-00ER45813-A001. M. F. C. and G. D. acknowledge support from the Department of Energy under Contract No. DE-AC05-00OR22725. The authors appreciate the help from Dr. J. M. Kikkawa with Hall effect measurement and insightful discussions with Dr. I.-W. Chen, Dr. Juraj Vavro, and Dr. Sergei V. Kalinin.

[1] P. A. Fleury, J. F. Scott, and J. M. Worlock, Phys. Rev. Lett. **21**, 16 (1968); H. Thomas and K. A. Müller, *ibid.* **21**, 1256 (1968).
[2] K. A. Müller, and H. Burkard, Phys. Rev. B **19**, 3593 (1979).
[3] K. A. Müller, W. Berlinger, and E. Tosatti, Z. Phys. B **84**, 277 (1991); R. Martonák and E. Tosatti, Solid State Commun. **92**, 167 (1994).
[4] J. F. Schooley and W. R. Hosler, Phys. Rev. Lett. **12**, 474 (1964); G. Binnig *et al.*, *ibid.* **45**, 1352 (1980).
[5] G. E. Pike and C. H. Seager, J. Appl. Phys. **50**, 3414 (1979).
[6] R. Shao, J. Vavro, and D. A. Bonnell, Appl. Phys. Lett. **85**, 561 (2004).
[7] J.-H. Hwang *et al.*, Appl. Phys. Lett. **76**, 2621 (2000); S. V. Kalinin and D. A. Bonnell, *ibid.* **78**, 1306 (2001); R. Shao and D. A. Bonnell, *ibid.* **85**, 4968 (2004).
[8] M. M. McGibbo., N. D. Browning, M. F. Chisholm, A. J. McGibbon, S. J. Pennycook, V. Ravikumar, and V. P. Dravid, Science **266**, 102 (1994).
[9] Q. D. Jiang, X. Q. Pan, and J. Zegenhagen, Phys. Rev. B **56**, 6947 (1997).
[10] M. Kim, G. Duscher, N. D. Browning, K. Sohlberg, S. T. Pantelides, S. J. Pennycook, Phys. Rev. Lett. **86**, 4056 (2001).
[11] Z. Zhang, W. Sigle, W. Kurtz, and M. Rühle, Phys. Rev. B **66**, 214112 (2002).
[12] J. Hemberger, P. Lunkenheimer, R. Viana, R. Böhmer, and A. Loidl, Phys. Rev. B **52**, 13 159 (1995).
[13] H. Uwe and T. Sakudo, Phys. Rev. B **13**, 271 (1976).
[14] O. Tikhomirov, H. Jiang, and J. Levy, Phys. Rev. Lett. **89**, 147601 (2002).
[15] S. J. Pennycook and L. A. Boatner, Nature (London) **336**, 565 (1988).
[16] H. P. R. Frederikse, W. R. Thurber, and W. R. Hosler, Phys. Rev. **134**, A442 (1964).
[17] O. N. Tufte and P. W. Chapman, Phys. Rev. **155**, 796 (1967).
[18] G. Kresse and J. Hafner, Phys. Rev. B **47**, R558 (1993); G. Kresse and J. Furthmüller, *ibid.* **54**, 11 169 (1996); G. Kresse and D. Joubert, *ibid.* **59**, 1758 (1999); P. E. Blöchl, *ibid.* **50**, 17 953 (1994).
[19] N. D. Browning *et al.*, Appl. Phys. Lett. **74**, 2638 (1999).
[20] J. Petzelt *et al.*, Phys. Rev. B **64**, 184111 (2001).
[21] K. Hayashi, T. Yamamoto, Y. Ikuhara, and T. Sakuma, J. Appl. Phys. **86**, 2909 (1999).
[22] D. A. Bonnell and S. V. Kalinin, Z. Metallkd. **94**, 188 (2003).
[23] H.-M. Christen *et al.*, Phys. Rev. B **49**, 12 095 (1994).
[24] J. H. Barrett, Phys. Rev. **86**, 118 (1952).